FOI-R--1171--SE
April 2005
ISSN 1650-1942
Scientific report

Ingvar Nedgård

A comparison of analysis methods for vehicle classification by laser vibrometry

Sensor Technology
SE-581 11 Linköping

Systems Technology
SE-172 90 Stockholm

SWEDISH DEFENCE RESEARCH AGENCY

Sensor Technology
SE-581 11 Linköping

Systems Technology
SE-172 90 Stockholm

FOI-R--1171--SE

April 2005

ISSN 1650-1942

Scientific report

Ingvar Nedgård

A comparison of analysis methods for vehicle classification by laser vibrometry

Issuing organization	Report number, ISRN	Report type
FOI – Swedish Defence Research Agency Sensor Technology SE-581 11 Linköping Systems Technology SE-172 90 Stockholm	FOI-R--1171--SE	Scientific report
	Research area code 4. C4ISR	
	Month year April 2005	**Project no.** E3059/E3965
	Customers code 5. Commissioned Research	
	Sub area code 42. Surveillance Sensors	

Author/s (editor/s)	Project manager
Ingvar Nedgård	Tomas Chevalier/Dietmar Letalick
	Approved by Lena Klasén
	Sponsoring agency Swedish Armed Forces
	Scientifically and technically responsible Anna Linderhed

Report title

A comparison of analysis methods for vehicle classification by laser vibrometry

Abstract (not more than 200 words)

In this report laser vibrometry data from six different vehicles are analysed by four different analysis methods. The vehicles are the track-laying vehicles Bv206, Strf90, T72, Strv121, and on wheels Tgb11 and Tglb30. The data is collected at tree different test sites, and in various conditions. The frequency modulated data is first preprocessed by peak detection, and transient reduction. Features are extracted from power spectral density spectra (PSD), autoregressive model parameters (AR), Morlet wavelet spectra, and by empirical mode decomposition (EMD), and Hilbert spectra. Six elements are used in each feature vector. The feature vectors of each vehicle are divided in reference data and test data. The test data is classified by Mahalanobis classification and associated to the nearest reference data class. All together 222 measurements are used. Best result is achieved by the EMD-method and 62% of the test signals are assigned to the right reference class in the six class case, without regard to differences in the engine rpm or surfaces illuminated. Feature vectors of dimension five are also classified. The best result is again achieved by the EMD-method but here only 56% of the test signals are assigned to the right reference class in the six class case. The focus here is primarily on the comparison of the analysis methods and it is suggested that a higher classification percentage could be achieved by testing one feature vector at a time leaving the rest to a better estimation of the mean and the covariance matrix of the reference class. Feature vector element values are not included in the appendices of the report but are available as a supplement.

Keywords

Time-frequency analysis, EMD, Morlet, AR, PSD, vibrometry, laser radar, Doppler, classification

Further bibliographic information	Language English
ISSN 1650-1942	**Pages** 32 p.
	Price acc. to pricelist

Utgivare	Rapportnummer, ISRN	Klassificering
Totalförsvarets Forskningsinstitut - FOI	FOI-R--1171--SE	Vetenskaplig rapport
Sensorteknik 581 11 Linköping	**Forskningsområde** 4. Spaning och ledning	
	Månad, år April 2005	**Projektnummer** E3059/E3965
Systemteknik 172 90 Stockholm	**Verksamhetsgren** 5. Uppdragsfinansierad verksamhet	
	Delområde 42. Spaningssensorer	

Författare/redaktör	Projektledare
Ingvar Nedgård	Tomas Chevalier/Dietmar Letalick
	Godkänd av Lena Klasén
	Uppdragsgivare/kundbeteckning FM
	Tekniskt och/eller vetenskapligt ansvarig Anna Linderhed

Rapportens titel (i översättning)

En jämförelse av analysmetoder för fordonsklassificering med laservibrometri

Sammanfattning (högst 200 ord)

Mätdata från sex olika fordon insamlade med laser vibrometer analyserades med fyra olika analysmetoder. Fordonen är de fyra bandfordonen Bv206, Strf90, T72, Strv121 och de två hjulfordonen Tgb11 ochTglb30. Mätdata insamlades vid tre olika platser och under varierande förhållanden. De frekvensmodulerade signalerna "demodulerades" genom detektion av maximala frekvenstoppen i spektrum från konsekutiva tidsfönster och signalen rensades sedan från transienta störningar. Karakteristiska egenskaper extraherades från effekttäthetspektra (PSD), autoregressiva modellparametrar (AR), Morlet vågformspektra och empirisk moduppdelning (EMD) följd av Hilbert spektra. Sex komponenter användes i varje särdragsvektor. Särdragsvektorerna för varje fordon delades upp I en grupp med referensdata och en grupp med testdata. Klassificeringen utfördes med Mahalanobis klassificering och testdata associerades till närmaste klass av referensdata. Totalt användes 222 mätsignaler. Bästa resultatet erhölls med EMD-metoden där 62 % av testsignalerna tilldelades rätt referensklass i fallet med sex fordonsklasser. Ingen uppdelning gjordes avseende variation av motorvarvtal eller vilka ytor på fordonet som belystes, och inte heller avseende infallsvinkeln mellan laserstrålen och fordonet. Klassificering utfördes också med fem komponenter i särdragsvektorerna. Bästa resultatet erhölls åter igen med EMD-metoden men då bara med 56 % av testsignalerna i rätt klass för fallet med sex fordonsklasser. Här har vi fokuserat på jämförelsen mellan analysmetoderna, men förmodligen kan en högre klassificeringsprocent uppnås om en särdragsvektor i taget testas då medelvektorn och covariansmatrisen för klassen kan bestämmas med högre noggrannhet. Särdragsvektorernas komponentvärden har ej tagits med i rapporten, men kan erhållas som bilaga.

Nyckelord

Tids-frekvensanalys, EMD, Morlet, AR, PSD, vibrometri, laserradar, Doppler, klassificering

Övriga bibliografiska uppgifter	Språk Engelska
ISSN 1650-1942	**Antal sidor:** 32 s.

Contents

Introduction 5
Physical signal model 5
Data preprocessing 5
Analysis methods 8
  Power Spectral Density (PSD) 8
  Autoregressive (AR) model 9
  Morlet Wavelet 9
  Empirical Mode Decomposition (EMD) 10
Classification 12
Results 12
Discussion 26
References 27
Appendix A 29
Appendix B 30
Appendix C 31
Appendix D 32

Introduction

Identification of military ground vehicles is an important issue in peace keeping and war situations. Many different techniques have been used to gain information about what is on the battlefield. Some work previously published at FOI involves images of vehicles from passive IR-sensors, and active 3D laser radar [17], and identification by seismic sensors [6]. Here we will concentrate on laser vibrometry, another interesting technique that has been reported to be promising for vehicle identification [4, 16].

The aim of this report is to briefly compare some analysis methods on real data from six different vehicles, four track-laying vehicles Bv206, Strf90, T72, Strv121, and two vehicles on wheels Tgb11 and Tglb30. The vehicles are illuminated by coherent laser radar at 1.55 µm and the returning signal is mixed down using an acoustic-optical heterodyne method. Then the carrier frequency only consists of the Doppler induced frequencies [13]. The data was made available by Dr. Dietmar Letalick and his group at the Division of Sensor Technology at the Defence Research Agency in Linköping. The measurements are conducted at different distance, at different illumination angle, on different surfaces on the vehicles and with the engine running at different revolutions per minute. Only measurements with the vehicles stationary are used. Some short data records, records with system error logged, and measurements at distance 1900 m where the laser probably missed the target, are excluded. The distance is determining the amount of the transmitted signal returned from the vehicle compared to the returned signal from the surroundings. Several surfaces can also be simultaneously illuminated and vibrate in different modes causing a lower signal-to-noise ratio [12]. The angle of incidence on the surface as well as the reflection property of the surface will have an impact on the reflected signal [8]. All together 222 measurements are used. The data is collected at tree different test sites, Kvarn May 2-3, 2002, Skövde June 12-13, 2002, and Älvdalen October 10, 2002.

Physical signal model

The engine force the body of the vehicle in vibration and an illuminated surface will lower and raise the frequency on the returning signal as the surface move away and toward the laser. Consequently, we will receive a frequency modulated (FM) return signal. A displacement of one millimeter per second will result in a frequency shift of the order 1 kHz. An additional trend in frequency shift will occur if the vehicle moves in a radial direction toward or away from the laser. This will result in larger frequency shift up to several MHz. A sinusoid model of the harmonically vibrating surface and the mixed down frequency modulated carrier signal is given in [13].

Data preprocessing

The traditional band pass/limiter can not be used here since there is an unstable carrier frequency in the mixed down signal [1].

Instead, the mixed down signal is divided into segments, windows each of the length 1024 samples and with no overlap. This is equivalent to a time segment of 0.4 ms for the T72 vehicle data and 1ms for data from the other vehicles. In every segment the power spectral density (PSD) is estimated via Welch's method [20].

Figure 1 shows a spectrogram from the mixed down signal of a Russian T72 tank. The signal is divided in segments of window length 1024 samples with no overlap. The frequency contents in the segments are determined in sequence by a length 1024 discrete Fourier transform.

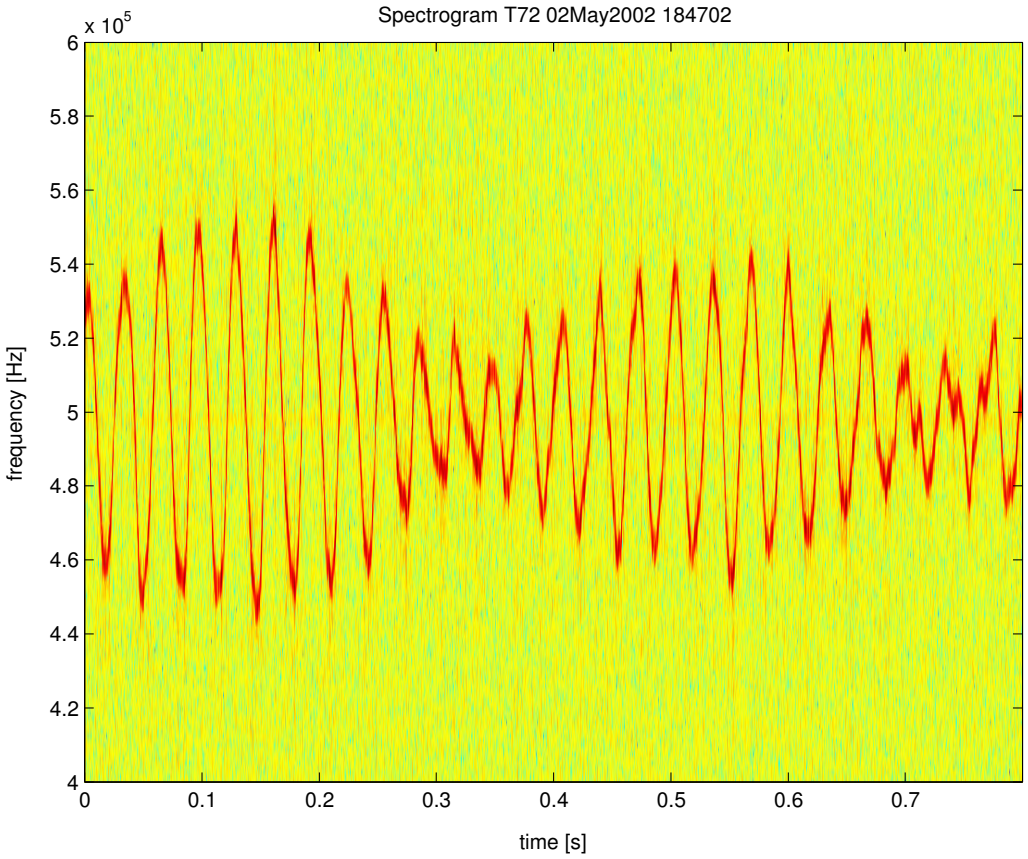

Figure 1. Spectrogram from the signal of a Russian T72 tank, NFFT=1024.

The instantaneous frequency of the mixed down signal is estimated from the PSD in each segment by peak detection [13] of the maximum power per unit frequency. Figure 2 shows the tracked time-frequency demodulated signal of the T72 tank from figure 1 with the mean frequency removed.

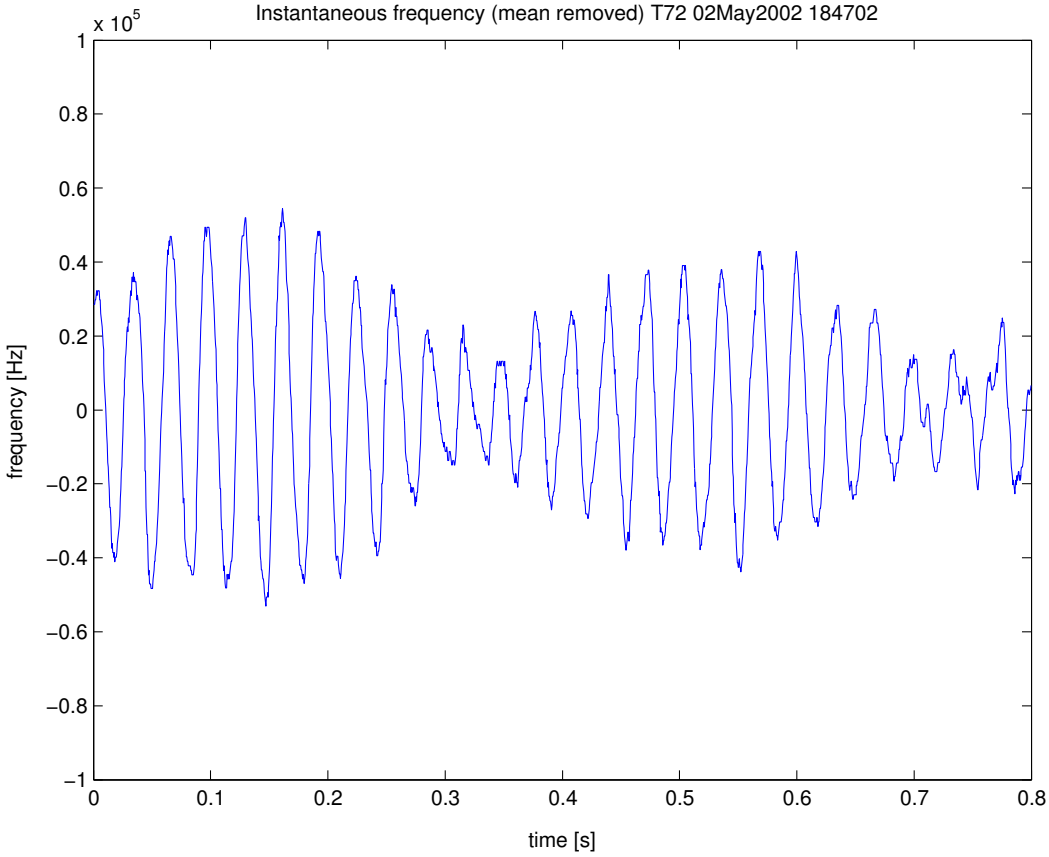

Figure 2. The time-frequency demodulated signal of the T72 tank with the mean frequency removed.

The sampling rate Fs of the mixed down signal, the size of the FFT transform and the associated frequency resolution in the Doppler shift is given in table 1 for the data from the different vehicles.

Vehicle	Test Site	Fs [MHz]	NFFT	Resolution [Hz]
Tgb11	Skövde	1.0	16384	61
Tglb30	Älvdalen	1.0	8192	122
Bv206	Älvdalen	1.0	8192	122
Strf90	Skövde	1.0	2048	488
T72	Kvarn	2.5	2048	1220
Strv121	Skövde	1.0	2048	488

Table1. Vehicle measurements sampling rate and resolution.

The length of the demodulated signals is 1953 samples (number of segments). The sampling frequency of the demodulated signals is 2441 Hz for the T72 vehicle signal and 977 Hz for the other vehicles. That is 0.8 second data records from the T72 tank and 2.0 second data records from the other vehicles. Transient disturbances in the demodulated signal are observed in some data files. Large transient values exceeding three standard deviations of the signal are replaced by the preceding sample.

Analysis methods

Four different feature extraction methods are used in analyzing the demodulated signals. The first is the power spectral density method which is the reference method we will compare to the other methods. The other methods are the autoregressive model, the Morlet wavelet and the empirical mode decomposition. The features of the last two methods are presented in more versions.

Power Spectral Density (PSD)

The laser radar is previously tested in a laboratory with two speakers used as targets [1] and up to a distance of 200 m. The speakers were vibrating at 85 Hz and at 125 Hz. The noise is not a large problem at this distance. However, as the distance increase the reflected signal energy will decrease and finally generate erroneous results. Analysis of the system limits due to noise is given by T. Carlsson and D. Letalick [2].

At the test sites a camera is used to direct the laser to the target. There are no accelerometer measurements on the vehicles to identify the features at the source, and therefore the "blind" analysis depend on the level of the returned target signal. The six largest peaks in the power spectral density of the demodulated signals are extracted to identify pattern of common frequencies in the classes. Figure 3 shows the peak pattern from Bv206. There are 34 demodulated signals each contributing their six largest peaks which means 204 observations.

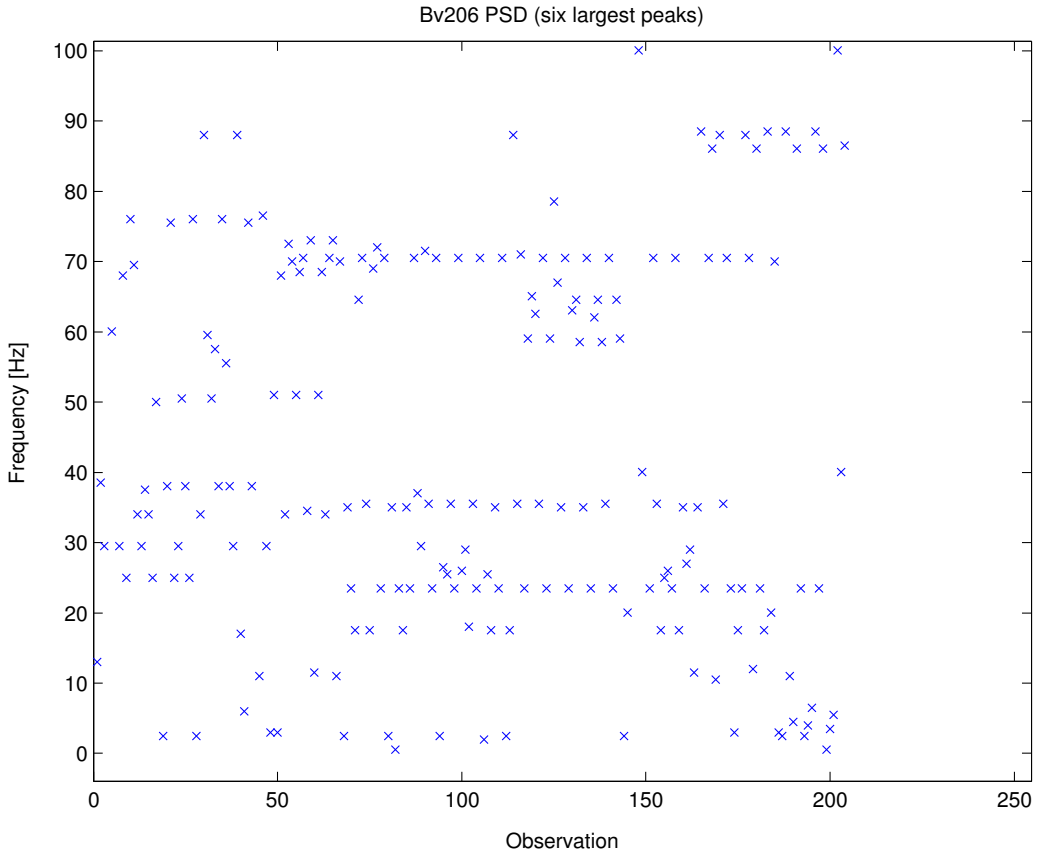

Figure 3. Peak pattern from Bv206, six largest peaks from each signal.

Typical frequencies are found for Bv206 at 24 Hz, 36 Hz, and 71 Hz. A summary of the most typical frequencies occurring for the vehicles are given in table 2.

Vehicle	Frequencies [Hz]
Tgb11	4-5, 26-34
Tglb30	2.5, 7.5, 23, 45
Bv206	24, 35-36, 71
Strf90	44-45, 89
T72	30-34, 60-65
Strv121	21, 41 ,82

Table 2. Most typical frequencies from PSD peaks.

The six frequencies of the largest PSD peaks in descending order are used as feature vector elements of the PSD method.

Autoregressive (AR) model

A six order AR model of the demodulated signal is estimated by the modified covariance method (forward-backward approach) [9, 11]. The autoregressive (AR) model is given by,

$$\sum_{i=0}^{6} a_i\, y(n-i) = e(n)$$

where a_i is the parameters of the model, $y(n)$ is the demodulated signal and $e(n)$ is the generating white stochastic process.

The six AR-parameters are used as feature vector elements of the AR method.

Morlet Wavelet

The demodulated signal caused by the vibrating surfaces is not known but it can be described by sinusoid transients of different frequencies and duration (see figure 2). This makes the wavelet transform with the Morlet base especially suitable for vibrometry signals [14].

The Morlet base is obtained from the function of a plane wave modulated by a Gaussian function,

$$\psi_0(\eta) = \pi^{-1/4} e^{i\omega_0\eta} e^{-\eta^2/2}$$

where η is a nondimensional ”time” parameter and ω_0 is the nondimensional frequency.

A MATLAB program from the University of Colorado [18] is used in the wavelet analysis. The spacing between discrete scales is 0.01 and the wave number parameter is 6.

The frequency corresponding to the time/scale indices are determined and the marginal frequency magnitudes are calculated as mean over time for each fixed frequency. Numerical differentiation and zero crossings are used to calculate the maxima of the marginal spectra. The maxima are sorted in descending magnitude order and the frequencies of the six largest peaks are selected as characteristic parameters. The frequencies are also used as feature vector elements sorted in descending frequency order.

Empirical Mode Decomposition (EMD)

The Fourier spectral analysis requires the system to be linear and the data must be strictly periodic or stationary. If not the resulting spectrum will make little physical sense. In practice, these assumptions are only approximations. Spurious harmonics and a wide frequency spectrum can occur when many Fourier components are added to simulate the non-stationary nature of the data. Empirical Mode Decomposition [7] is an analysis method that in many aspects gives a better understanding of the physics behind the signals. Because of its ability to describe short time changes in frequencies that can not be resolved by Fourier spectral analysis it can be used for nonlinear and non-stationary time series analysis. The method is based on a technique to divide the signal in its Intrinsic Mode Functions (IMF).

An IMF satisfies two conditions:

1. In the whole data set, the number of extrema and the number of zero crossings must either equal or differ at most by one.
2. At any point, the mean value of the envelope defined by the local maxima and the envelope defined by the local minima is zero.

The process used in EMD is called the sifting process.
The decomposition is based on the assumptions:

1. The signal has at least two extrema – one maximum and one minimum.
2. The characteristic time scale is defined by the time lapse between the extrema.
3. If the data were totally devoid of extrema but contained only inflection points, then it can be differentiated once or more times to reveal the extrema. Final results can be obtained by integration(s) of the components.

The sifting process is an iterative process and it can be described as follows:

- Identify the local maxima and minima.
- All the local maxima are connected by a cubic spline line as the upper envelope.
- All the local minima are connected by a cubic spline line as the lower envelope.

The upper and lower envelopes should cover all the data between them. Their mean is designated as m_1, and the difference between the data and m_1 is the first component, h_1 i.e.

$$X(t) - m_1 = h_1$$

There might still be negative local maxima and positive minima suggesting riding waves. If h_1 is not an IMF we repeat the procedure with h_1 instead of the data. We can repeat the sifting procedure k times, until h_{1k} is an IMF, that is

$$h_{1(k-1)} - m_{1k} = h_{1k}$$

Then, the first IMF component from the data is designated as

$$c_1 = h_{1k}$$

We can separate c_1 from the rest of the data by,

$$X(t) - c_1 = r_1$$

We finally obtain,

$$X(t) = \sum_{i=1}^{n} c_i + r_n$$

where the signal is decomposed into n-empirical modes, and a residue, r_n which can be either the mean trend or a constant.

The different modes might contain oscillations of the same scale, but signals of the same time scale would never occur at the same locations in two different IMF components. Now, we can apply the Hilbert transform to each IMF component and compute the instantaneous frequency and the instantaneous amplitude from the analytic signal. The instantaneous amplitude and frequency are distributed over time and the amplitude density is a measure of the frequency presence in a time interval.

Serious problems of the spline fitting can occur near the ends and corrupt especially the low-frequency components. Huang et.al. [7] have devised a numerical method, adding two characteristic waves at either end, to eliminate these end effects. The Hilbert transform also have end effects and again characteristic waves can be used to eliminate these end effects. These attached waves begin at the slightly enlarged data set with zero, and likewise end it with a zero level. Another complication is that the envelope mean may still be different from the true local mean for nonlinear data no matter how many times the data are sifted. The choice of stop criteria in the sifting process will also determine the time of computation.

A MATLAB-program from Laboratoire de Physique, Lyon, France [15] is used in the EMD analysis. The characteristic parameters are computed from the median of the instantaneous frequency obtained from the first six modes. These frequencies are used as feature vector elements sorted in descending frequency order and in descending marginal median amplitude order.

The demodulated signal is also divided in windows each of length 400 samples. The Hilbert-Huang-Transform is applied as above on each window and the mean of the median of the instantaneous frequencies obtained are used as feature vector elements. These are only sorted in descending frequency order.

Classification

Signal detection and signal classification can both be regarded as hypothesis tests [19]. In detection [5] we decide if a signal is present or not and in classification we decide if some feature parameters belong to one class or not. A comparison of the ability of the different analysis methods to separate the vehicles in different classes is made by Mahalanobis classification [10, 3].

The Mahalanobis distance r from the feature vector x to the mean vector m_x is given by,

$$r^2 = (x - m_x)^T C_x^{-1} (x - m_x)$$

where C_x is the covariance matrix for *x*. One can use the Mahalanobis distance in a minimum-distance classifier as follows. Let $m_1, m_2, \ldots, m_c$ be the means for the *c* classes, and let $C_1, C_2, \ldots, C_c$ be the corresponding covariance matrices. We assign a feature vector x to the class for which the Mahalanobis distance is minimum.

The feature vector data from each vehicle is divided in two groups, one containing the reference data and the other containing the test data. For every test vector x the distance to the mean reference vector m_x of each class is calculated and x is assigned to the nearest class. This procedure is performed on all the analysis methods.

Let n be the number of reference vectors in a class and let d be the number of elements in the feature vector. If $n < d+1$, the matrix C is singular. This is very bad since we need to invert C to form the Mahalanobis distance.

Even if $n > d+1$ we should not expect to get a good estimate for C until our number n of reference vectors in the class gets close to the number $d(d-1)/2$ of independent elements in C (symmetric). The classification is performed for $d = 6$ (n close to 15) and $d = 5$ (n close to 10).

Results

Altogether, 222 measurements are used in this report distributed on Tgb11 (42), Tglb30 (21), Bv206 (34), Strf90 (21), Strv121 (48) and T72 (56). The same data files are used by all analysis methods. Tables of the extracted frequencies by the *PSD* analysis method is given in appendix A. The frequencies are collected in a vector for each vehicle and frequencies up to 400 Hz are presented as histograms of bin width 1 Hz in figure 4.

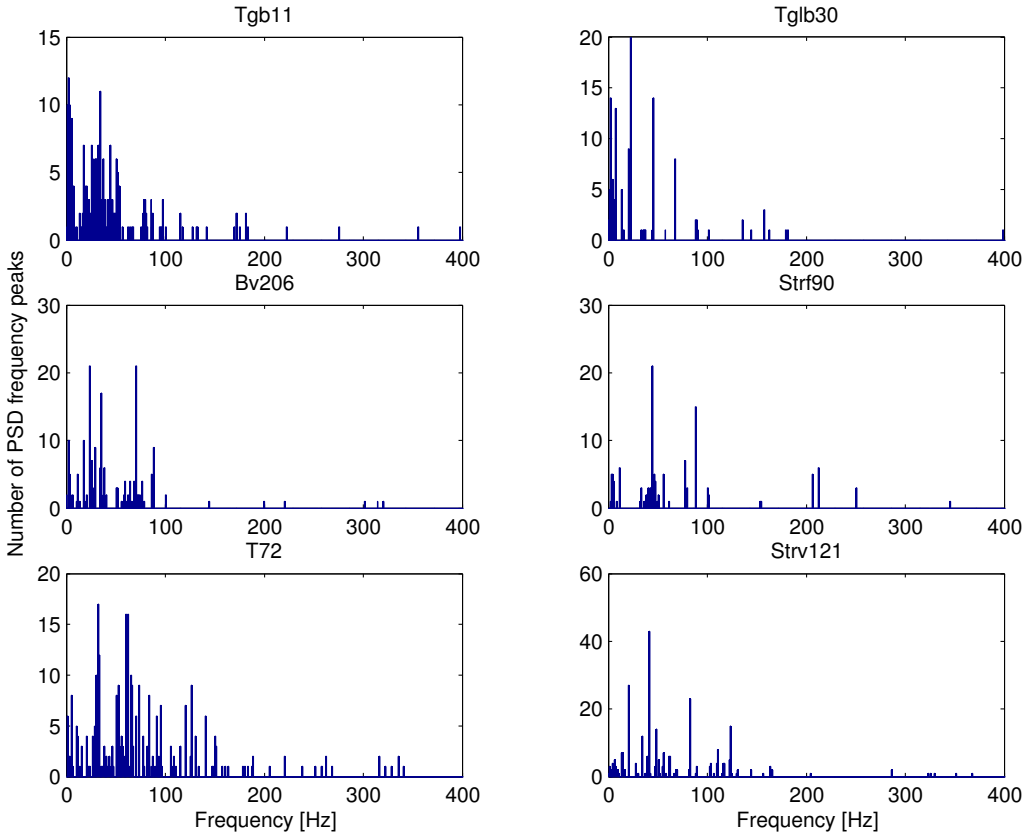

Figure 4. Number of frequency peaks in 1 Hz interval from the PSD analysis.

Tables of the parameters of the *AR* method and the extracted frequencies by the *Morlet wavelet* analysis method is given in appendix B. The mean of the Morlet wavelet amplitude for the Tgb11 vehicle versus frequency is given in figure 5. We observe a concentration of energy at 30-35 Hz that might be due to surface vibration on the vehicle.

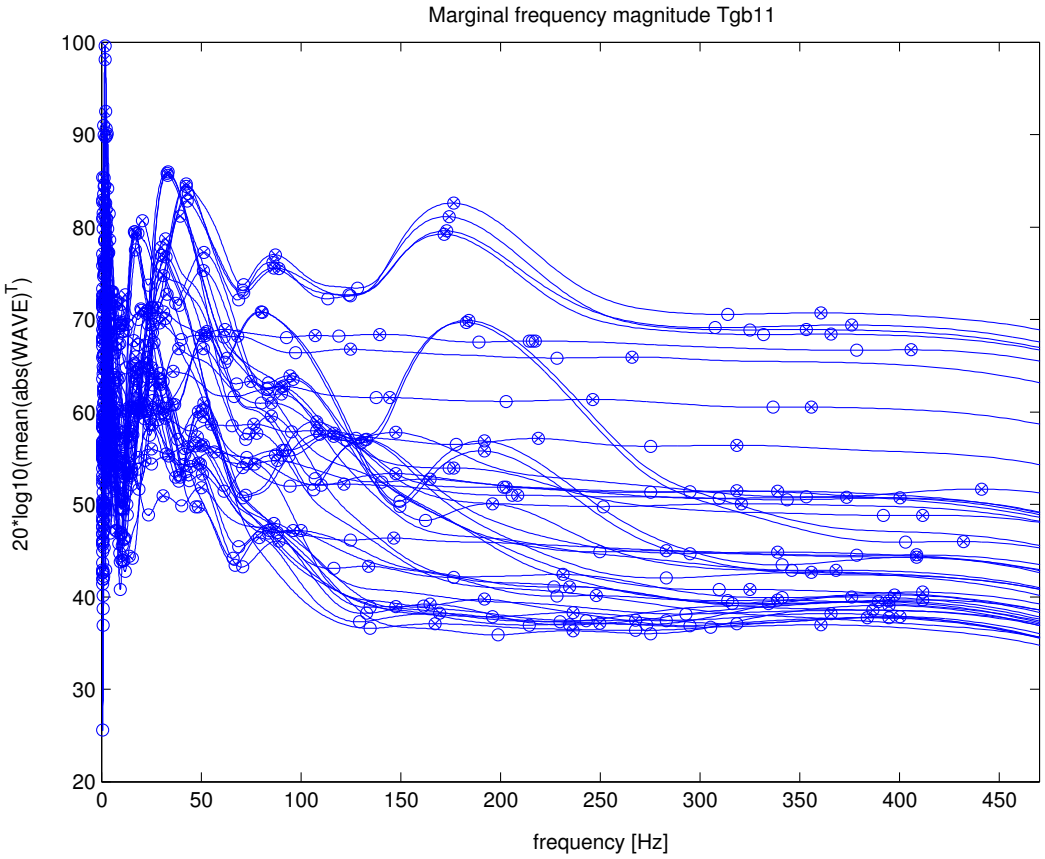

Figure 5. Morlet wavelet, marginal frequency magnitude versus frequency (Tgb11).

The mean of the Morlet wavelet amplitude for the Tglb30 vehicle versus frequency is given in figure 6. Two distinct peaks at 23 Hz and 45 Hz are observed that might be due to surface vibration on the vehicle.

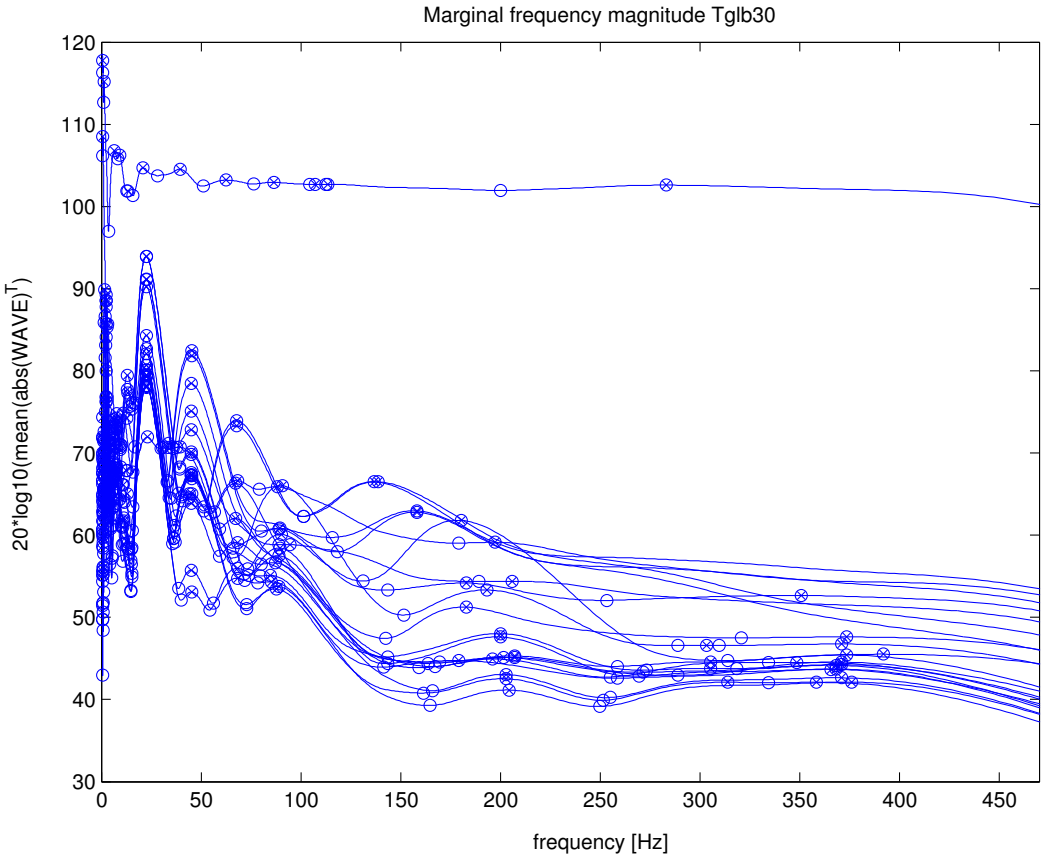

Figure 6. Morlet wavelet, marginal frequency magnitude versus frequency (Tglb30).

The mean of the Morlet wavelet amplitude for the Bv206 vehicle versus frequency is given in figure 7. Frequency peaks at 36 Hz and 71 Hz that might be due to surface vibration on the vehicle are clearly seen.

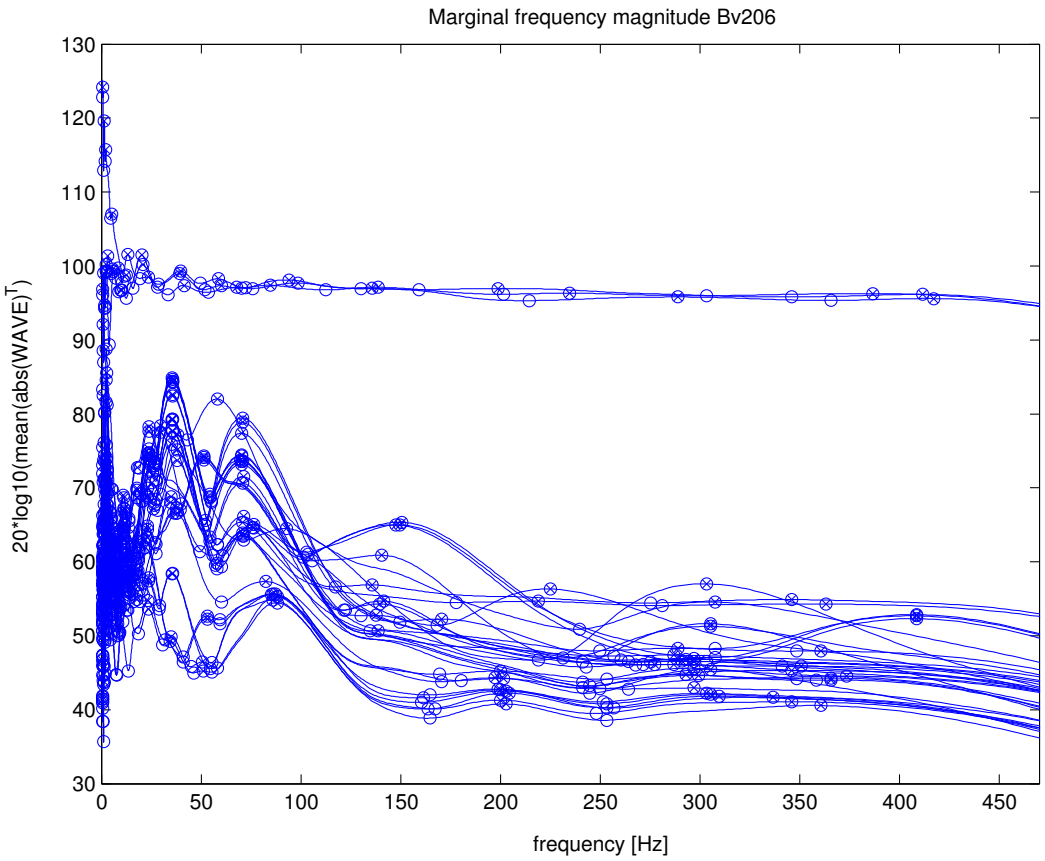

Figure 7. Morlet wavelet, marginal frequency magnitude versus frequency (Bv206).

The mean of the Morlet wavelet amplitude for the Strf90 vehicle versus frequency is given in figure 8. Two distinct peaks at 44 Hz and 88 Hz are observed that might be due to surface vibration on the vehicle.

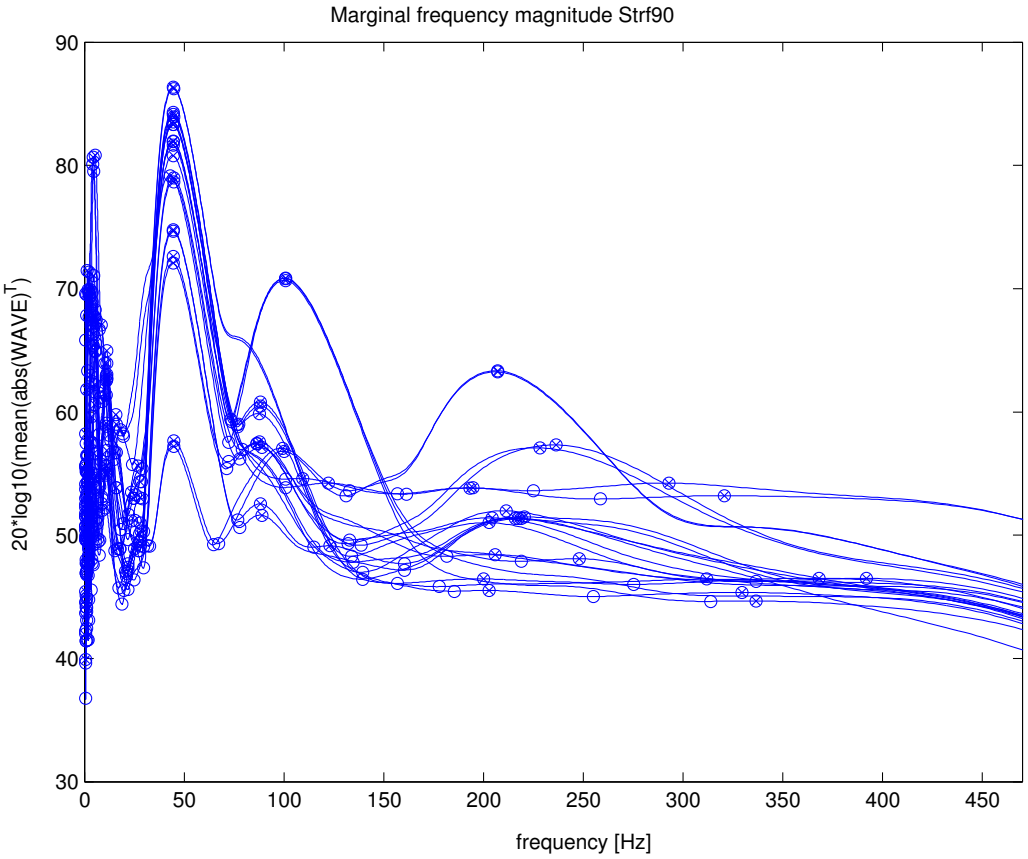

Figure 8. Morlet wavelet, marginal frequency magnitude versus frequency (Strf90).

The mean of the Morlet wavelet amplitude for the T72 vehicle versus frequency is given in figure 9. We observe a concentration of energy at 34 Hz and 67 Hz that might be due to surface vibration on the vehicle.

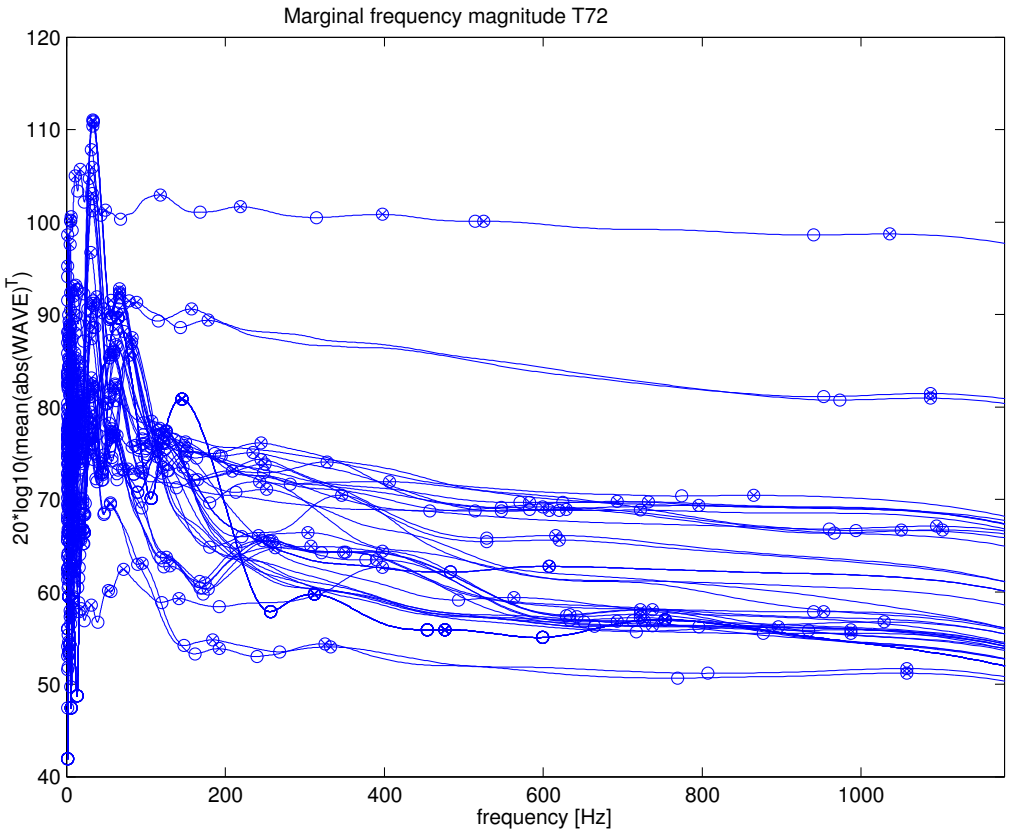

Figure 9. Morlet wavelet, marginal frequency magnitude versus frequency (T72).

The mean of the Morlet wavelet amplitude for the Strv121 vehicle versus frequency is given in figure 10. Frequency peaks at 41 Hz and 82 Hz that might be due to surface vibration on the vehicle can be observed.

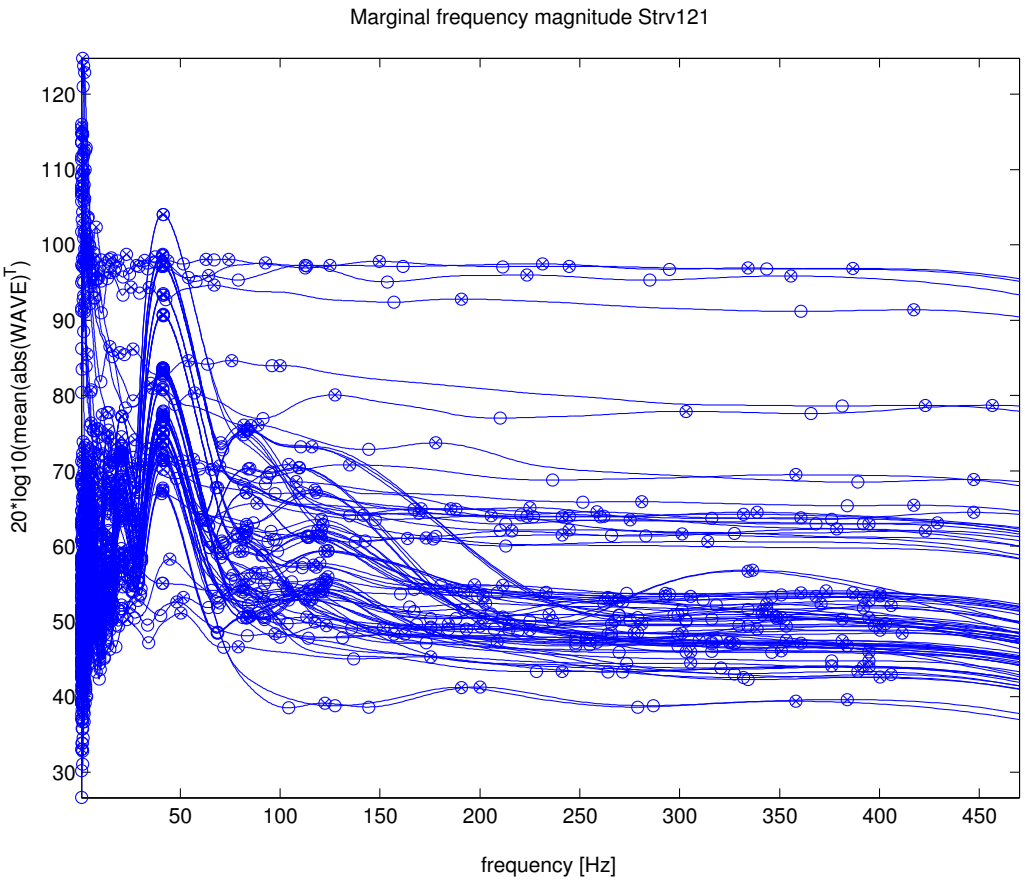

Figure 10. Morlet wavelet, marginal frequency magnitude versus frequency (Strv121).
.

Two methods are used to analyse the signals by *EMD* and the *Hilbert spectrum*:

1. Analyse the whole demodulated signal. Marginal frequencies and marginal amplitudes are calculated as median of the distribution.
2. Analyse consecutive 400 sample windows without overlap. Marginal frequencies and marginal amplitudes are calculated as median of the distribution in each window. The mean of the marginal frequencies and the mean of the marginal amplitudes are then calculated.

Tables of the extracted frequencies of the *EMD* method 1 is given in appendix C and the extracted frequencies by the *EMD* analysis method 2 is given in appendix D.

The highest frequency that can be extracted by the EMD methods for the 0.8 second data records of the T72 vehicle is 610 Hz, and the lowest frequency is 1.25 Hz for method 1 and 6.10 Hz for the window method 2.

The highest frequency that can be extracted by the EMD methods for the 2 second data records of the other vehicles is 244 Hz, and the lowest frequency is 0.5 Hz for method 1 and 2.44 Hz for the window method 2.

The result of the classification by the different methods is shown by assignment matrices. The classification is first performed with feature vectors of dimension $d = 6$ and then with feature vectors of dimension $d = 5$ to see if any improvement can be made in the estimate of the covariance C_x. The result of course depends on the number of classes used, the number of elements in the feature vector; the elements target significance, and the number of reference feature vectors available to calculate the covariance matrix. The mean window EMD-method with the feature vector elements in descending frequency order $d = 6$ is shown in table 3.

Test => ***Reference***	***Tgb11***	***Tglb30***	***T72***	***Strf90***	***Strv121***	***Bv206***
Tgb11	15	2	1	0	4	3
Tglb30	0	2	0	1	2	2
T72	0	0	27	0	0	0
Strf90	1	2	0	5	2	4
Strv121	2	3	0	4	15	4
Bv206	3	1	0	0	1	4
∑	21	10	28	10	24	17

Table 3. Mean window EMD-method frequency order $d = 6$.

This method assigns 68 out of the 110 test signals (62 %) to the right reference class. Out of the two vehicles on wheels 19 of the 31 test signals (61 %) are assigned to the wheel class, and out of the four track-laying vehicles 66 of the 79 test signals (84 %) are assigned to the track-laying vehicles.

The EMD-method on the whole demodulated signal with the feature vector elements in descending amplitude order, $d = 6$ is shown in table 4.

Test => ***Reference***	***Tgb11***	***Tglb30***	***T72***	***Strf90***	***Strv121***	***Bv206***
Tgb11	9	5	0	4	2	4
Tglb30	5	3	1	0	0	4
T72	0	1	26	0	0	0
Strf90	1	0	0	1	4	1
Strv121	4	0	1	4	16	7
Bv206	2	1	0	1	2	1
∑	21	10	28	10	24	17

Table 4. EMD-method amplitude order $d = 6$.

This method assigns 56 out of the 110 test signals (51 %) to the right reference class. Out of the two vehicles on wheels 22 of the 31 test signals (71 %) are assigned to the wheel class, and out of the four track-laying vehicles 64 of the 79 test signals (81 %) are assigned to the track-laying vehicles.

The EMD-method on the whole demodulated signal with the feature vector elements in descending frequency order, $d = 6$ is shown in table 5.

Test => ***Reference***	***Tgb11***	***Tglb30***	***T72***	***Strf90***	***Strv121***	***Bv206***
Tgb11	12	2	1	2	2	3
Tglb30	2	4	0	3	4	0
T72	0	0	27	0	0	0
Strf90	0	0	0	0	0	0
Strv121	3	3	0	3	14	3
Bv206	4	1	0	2	4	11
∑	21	10	28	10	24	17

Table 5. EMD-method frequency order $d = 6$.

This method assigns 68 out of the 110 test signals (62 %) to the right reference class. Out of the two vehicles on wheels 20 of the 31 test signals (65 %) are assigned to the wheel class, and out of the four track-laying vehicles 64 of the 79 test signals (81 %) are assigned to the track-laying vehicles.

The AR-method on the whole demodulated signal with the AR-parameters (leading 1 excluded) as feature vector elements, $d = 6$ is shown in table 6.

Test => ***Reference***	***Tgb11***	***Tglb30***	***T72***	***Strf90***	***Strv121***	***Bv206***
Tgb11	11	3	9	1	3	1
Tglb30	1	5	0	0	2	2
T72	4	0	14	0	1	0
Strf90	0	0	0	5	0	0
Strv121	2	0	0	3	13	1
Bv206	3	2	5	1	5	13
∑	21	10	28	10	24	17

Table 6. AR-method $d = 6$.

This method assigns 61 out of the 110 test signals (55 %) to the right reference class. Out of the two vehicles on wheels 20 of the 31 test signals (65 %) are assigned to the wheel class, and out of the four track-laying vehicles 61 of the 79 test signals (77 %) are assigned to the track-laying vehicles.

The Morlet-method on the whole demodulated signal with the feature vector elements in descending amplitude order, $d = 6$ is shown in table 7.

Test => Reference	Tgb11	Tglb30	T72	Strf90	Strv121	Bv206
Tgb11	10	6	7	2	7	5
Tglb30	0	0	0	0	0	0
T72	3	1	19	0	2	3
Strf90	1	0	1	6	2	4
Strv121	3	2	0	2	11	1
Bv206	4	1	1	0	2	4
∑	21	10	28	10	24	17

Table7. Morlet-method amplitude order $d = 6$.

This method assigns 50 out of the 110 test signals (45 %) to the right reference class. Out of the two vehicles on wheels 16 of the 31 test signals (52 %) are assigned to the wheel class, and out of the four track-laying vehicles 58 of the 79 test signals (73 %) are assigned to the track-laying vehicles.

The Morlet-method on the whole demodulated signal with the feature vector elements in descending frequency order, $d = 6$ is shown in table 8.

Test => Reference	Tgb11	Tglb30	T72	Strf90	Strv121	Bv206
Tgb11	6	3	1	2	2	3
Tglb30	0	0	0	0	0	0
T72	4	2	19	3	9	4
Strf90	4	0	1	4	2	3
Strv121	3	5	3	1	7	1
Bv206	4	0	4	0	4	6
∑	21	10	28	10	24	17

Table 8. Morlet-method frequency order $d = 6$.

This method assigns 42 out of the 110 test signals (38 %) to the right reference class. Out of the two vehicles on wheels 9 of the 31 test signals (29 %) are assigned to the wheel class, and out of the four track-laying vehicles 71 of the 79 test signals (90 %) are assigned to the track-laying vehicles.

The PSD-method on the whole demodulated signal with the feature vector elements in descending energy density order, $d = 6$ is shown in table 9.

Test => ***Reference***	***Tgb11***	***Tglb30***	***T72***	***Strf90***	***Strv121***	***Bv206***
Tgb11	9	6	5	6	1	4
Tglb30	0	1	1	0	0	0
T72	3	1	15	2	7	6
Strf90	1	0	1	0	1	0
Strv121	3	2	2	0	11	1
Bv206	5	0	4	2	4	6
∑	21	10	28	10	24	17

Table 9. PSD-method $d = 6$.

The PSD-method assigns 42 out of the 110 test signals (38 %) to the right reference class. Out of the two vehicles on wheels 16 of the 31 test signals (52 %) are assigned to the wheel class, and out of the four track-laying vehicles 62 of the 79 test signals (78 %) are assigned to the track-laying vehicles.

The mean window EMD-method with the feature vector elements in descending frequency order $d = 5$ is shown in table 10.

Test => ***Reference***	***Tgb11***	***Tglb30***	***T72***	***Strf90***	***Strv121***	***Bv206***
Tgb11	11	2	1	0	3	2
Tglb30	2	2	0	1	3	1
T72	0	0	27	0	0	0
Strf90	3	2	0	5	2	4
Strv121	2	2	0	4	13	6
Bv206	3	2	0	0	3	4
∑	21	10	28	10	24	17

Table 10. Mean window EMD-method frequency order $d = 5$.

This method assigns 62 out of the 110 test signals (56 %) to the right reference class. Out of the two vehicles on wheels 17 of the 31 test signals (55 %) are assigned to the wheel class, and out of the four track-laying vehicles 68 of the 79 test signals (86 %) are assigned to the track-laying vehicles.

The EMD-method on the whole demodulated signal with the feature vector elements in descending amplitude order, $d = 5$ is shown in table 11.

Test => ***Reference***	***Tgb11***	***Tglb30***	***T72***	***Strf90***	***Strv121***	***Bv206***
Tgb11	10	6	1	4	1	5
Tglb30	2	3	0	0	0	1
T72	4	1	27	1	6	3
Strf90	0	0	0	2	6	1
Strv121	4	0	0	3	11	7
Bv206	1	0	0	0	0	0
∑	21	10	28	10	24	17

Table 11. EMD-method amplitude order $d = 5$.

This method assigns 53 out of the 110 test signals (48 %) to the right reference class. Out of the two vehicles on wheels 21 of the 31 test signals (68 %) are assigned to the wheel class, and out of the four track-laying vehicles 67 of the 79 test signals (85 %) are assigned to the track-laying vehicles.

The EMD-method on the whole demodulated signal with the feature vector elements in descending frequency order, $d = 5$ is shown in table 12.

Test => ***Reference***	***Tgb11***	***Tglb30***	***T72***	***Strf90***	***Strv121***	***Bv206***
Tgb11	9	2	1	1	1	3
Tglb30	4	4	0	2	7	1
T72	0	0	27	0	0	0
Strf90	0	1	0	1	1	0
Strv121	4	2	0	4	12	6
Bv206	4	1	0	2	3	7
∑	21	10	28	10	24	17

Table 12. EMD-method frequency order $d = 5$.

This method assigns 60 out of the 110 test signals (55 %) to the right reference class. Out of the two vehicles on wheels 19 of the 31 test signals (61 %) are assigned to the wheel class, and out of the four track-laying vehicles 63 of the 79 test signals (80 %) are assigned to the track-laying vehicles.

The AR-method on the whole demodulated signal with the AR-parameters (leading 1 excluded) as feature vector elements, $d = 5$ is shown in table 13.

Test => ***Reference***	***Tgb11***	***Tglb30***	***T72***	***Strf90***	***Strv121***	***Bv206***
Tgb11	9	2	9	0	5	1
Tglb30	2	5	2	2	6	4
T72	3	1	12	1	1	0
Strf90	1	0	0	6	0	0
Strv121	2	0	0	0	10	1
Bv206	4	2	5	1	2	11
∑	21	10	28	10	24	17

Table 13. AR-method $d = 5$.

This method assigns 53 out of the 110 test signals (48 %) to the right reference class. Out of the two vehicles on wheels 18 of the 31 test signals (58 %) are assigned to the wheel class, and out of the four track-laying vehicles 50 of the 79 test signals (63 %) are assigned to the track-laying vehicles.

The Morlet-method on the whole demodulated signal with the feature vector elements in descending amplitude order, $d = 5$ is shown in table 14.

Test => ***Reference***	***Tgb11***	***Tglb30***	***T72***	***Strf90***	***Strv121***	***Bv206***
Tgb11	9	7	6	1	6	5
Tglb30	0	0	0	0	0	0
T72	3	1	18	0	4	3
Strf90	1	0	1	3	1	4
Strv121	3	2	0	4	11	1
Bv206	5	0	3	2	2	4
∑	21	10	28	10	24	17

Table 14. Morlet-method amplitude order $d = 5$.

This method assigns 45 out of the 110 test signals (41 %) to the right reference class. Out of the two vehicles on wheels 17 of the 31 test signals (55 %) are assigned to the wheel class, and out of the four track-laying vehicles 61 of the 79 test signals (77 %) are assigned to the track-laying vehicles.

The Morlet-method on the whole demodulated signal with the feature vector elements in descending frequency order, $d = 5$ is shown in table 15.

Test => ***Reference***	***Tgb11***	***Tglb30***	***T72***	***Strf90***	***Strv121***	***Bv206***
Tgb11	8	3	1	2	3	3
Tglb30	0	2	0	0	0	0
T72	3	0	19	2	4	1
Strf90	4	0	1	4	1	3
Strv121	3	3	3	2	8	3
Bv206	3	2	4	0	8	7
∑	21	10	28	10	24	17

Table 15. Morlet-method frequency order $d = 5$.

This method assigns 48 out of the 110 test signals (44 %) to the right reference class. Out of the two vehicles on wheels 13 of the 31 test signals (42 %) are assigned to the wheel class, and out of the four track-laying vehicles 70 of the 79 test signals (89 %) are assigned to the track-laying vehicles.

The PSD-method on the whole demodulated signal with the feature vector elements in descending energy density order, $d = 5$ is shown in table 16.

Test => ***Reference***	***Tgb11***	***Tglb30***	***T72***	***Strf90***	***Strv121***	***Bv206***
Tgb11	14	7	6	6	3	6
Tglb30	0	1	1	0	0	0
T72	2	2	14	2	5	4
Strf90	1	0	2	0	1	0
Strv121	1	0	1	1	11	1
Bv206	3	0	4	1	4	6
∑	21	10	28	10	24	17

Table 16. PSD-method $d = 5$.

The PSD-method assigns 46 out of the 110 test signals (42 %) to the right reference class. Out of the two vehicles on wheels 22 of the 31 test signals (71 %) are assigned to the wheel class, and out of the four track-laying vehicles 57 of the 79 test signals (72 %) are assigned to the track-laying vehicles.

Discussion

In a simplified model a surface on a vehicle can be regarded as a forced oscillator. The surface is forced to oscillate at the same frequency as the engine and the amplitude of the surface vibration depend on the number of revolutions. This means that the magnitude of the demodulated signal will fluctuate depending on the engine frequency. The mean window EMD-method and the EMD-method frequency order are the best of these methods to deal with this situation. Both methods assigned 62 % of the test signals to the right reference class with feature vectors of dimension $d = 6$ in the six class case. All methods but Morlet-method

frequency order and PSD-method performed better with $d = 6$ compared to $d = 5$ in the six class case.

If we reduce the classification to a two class problem we observe from table 3 (mean window EMD-method) that 61% of the vehicles on wheels are assigned to the wheeled class and 84% of the track-laying vehicles are assigned to the track-laying class. As might be expected for all methods the track-laying vehicles have a higher classification rate.

In more detail 71% of Tgb11, 40% of Tglb30, 96% of T72, 90% of Strf90, 75% of Strv121, and 71% of Bv206 are assigned to the right class in the two class problem. We can see that the motor lorry Tglb30 is mistaken for a track-laying vehicle.

The number of significant feature elements in the target feature vector is estimated from the power spectral density (see figure 3). No separate noise measurements are made.

Note that the analysis is made at different engine rpm, different illumination angle, different illuminated surface, and different distance to the vehicle. These circumstances contribute to divergence in the feature elements and influence the classification result. In the case when the number of feature vectors is few the estimation of the covariance matrix also can be done in a bootstrap manner. However, the main goal here is to compare the analysis methods and the elements of the feature vectors. The result is in favour for the EMD-method which has been reported to perform better on non-stationary signals than methods based on the periodic or stationary condition.

If the number of feature vectors is large a neural network can be trained to separate the vehicles in different classes.

References

[1] T. Carlsson. *Software signal processing. Scanning laser radar vibrometer at 1.55 μm.* FOI-D--0027—SE, November 2001.

[2] T. Carlsson, D. Letalick. *System setup and characterization – Laser radar vibrometer at 1.55 μm.* FOI-D—0028—SE, November 2001.

[3] R. O. Duda, P. E. Hart. *Pattern Classification and Scene Analysis.* Wiley-Interscience, New York, 1973.

[4] J. Geurts, D. Ruck, S. Rogers, M. Oxley, D. Barr. *Autonomous Target Recognition Using Remotely Sensed Surface Vibration Measurements.* SPIE Proceedings Vol. 1955, 1993.

[5] S. Haykin. *Adaptive Filter Theory.* Prentice-Hall, Inc., New Jersey 1996.

[6] I. Hansson, I. Nedgård, B. Nilsson. *Seismiska sensorer för spaning mot fordon och helikopter – utvärdering av fältförsök i Skövde 1984.* FOA Rapport, CH 20273-D4, Juni 1986.

[7] N. E. Huang, Z. Shen, S. R. Long, M. C. Wu, H. H. Shih, Q. Zheng, N-C. Yen, C. C. Tung and H. H. Liu. *The empirical mode decomposition and the Hilbert spectrum for nonlinear and non-stationary time series analysis*. Proc. R. Soc. Lond. A (1998) 454, 903-995.

[8] D. Letalick, I. Renhorn I., C. Karlsson. *Koherent ladarteknik vid 1,55 µm – En projektrapportering.* FOA-R--96-00317-3.1—SE, Oktober 1996.

[9] L. Ljung. *System Identification Theory for the User.* Prentice-Hall, Inc., New Jersey 1987.

[10] P. C. Mahalanobis. *On the generalized distance in statistics.* Proc. Natl. Institute of Science of India 2: 49-55, 1936.

[11] S. L. Marple, Jr. *Digital Spectral Analysis with Applications.* Prentice-Hall, New Jersey, 1987.

[12] M. Millnert. *Robust coherent laser radar design and signal processing for vibrometry.* SPIE Proceedings Vol. 2748, Laser Radar Technology and Applications, April 1996, Orlando, FL, USA.

[13] H. Nordin, C. Carlsson, C. Karlsson, D. Letalick. *Signal processing in laser radar vibrometry: A comparison of two frequency demodulation methods.* FOA-R--96-00333-3.1—SE, December 1996.

[14] M. I. Plett. *Ultrasonic Arterial Vibrometry with Wavelet Based Detection and Estimation.* University of Washington 2000.

[15] G. Rilling, P. Flandrin, P. Gonçalvès. *EMD MATLAB-kod.* Laboratoire de Physique, Lyon, France, URL: http://perso.ens-lyon.fr/patrick.flandrin/emd.html.

[16] M. R. Stevens, M. Snorrason, D. Petrovich. *Laser Vibrometry for Target Classification.* Proceedings of SPIE, Volume 4726, AeroSense, Orlando, FL (April, 2002).

[17] T. Svensson, H. Larsson, L. Klasén, M. Henriksson, T. Carlsson, I. Nedgård, D. Letalick, M. Elmquist, G. Carlsson och S. Cronström. *Prov i Kvarn med passiva och aktiva optroniska sensorsystem.* FOI-R--0740--SE, December 2002, ISSN 1650-1942.

[18] C. Torrence and G. P. Compo. *A Practical Guide to Wavelet Analysis.* Bulletin of the American Meteorological Society, Vol. 79, No. 1, January 1998.

[19] H. L. Van Trees. *Detection, Estimation and Modulation Theory,* part I, Wiley, New York, 1968.

[20] P. D. Welch. *The Use of Fast Fourier Transform for the Estimation of Power Spectra: A Method Based on Time Averaging Over Short, Modified Periodograms.* IEEE Trans. Audio Electroacoust. Vol. AU-15, June 1967.

Appendix A

Power Spectral Density: The table contains a vehicle identifier, date and time when the data is collected followed by the frequencies in Hz for the six largest peaks and their relative magnitude.

Appendix B

Autoregressive model and Morlet Wavelet: The table contains a vehicle identifier, date and time when the data is collected followed by the frequency of the maximal Morlet Wavelet peak in Hz. On the same row the six AR-parameters are given without the leading one. The next row contains the marginal frequencies of the six largest Morlet Wavelet peaks sorted in descending magnitude order.

Appendix C

Empirical Mode Decomposition (of the whole signal): The table contains a vehicle identifier, date and time when the data is collected followed by the median frequency of the instantaneous frequency obtained from each of the first ten modes. The frequencies are sorted in descending marginal median amplitude order and the relative amplitudes are given on the second row. Zero frequency and amplitude indicates less than ten modes.

Appendix D

Empirical Mode Decomposition (of 400 sample windows of the signal): The table contains a vehicle identifier, date and time when the data is collected followed by the mean value (from each of the first six modes) of the medians of the instantaneous frequencies obtained from the windows of the signal. The frequencies are sorted in descending mean frequency value order. The standard deviations are given on the second row. Zero mean frequency and standard deviation indicates less than six modes.